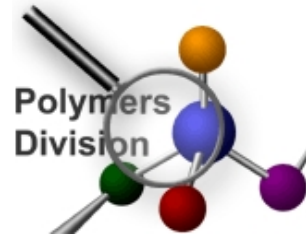


2010 NIST Diffusion Workshop, Gaithersburg, MD

Phase-Field Simulation of Line Edge Roughness in Block Copolymer Resists

Gus Bosse*



NIST
National Institute of
Standards and Technology
U.S. Department of Commerce

23 March 2010

*E-mail: august.bosse@nist.gov.

Background and Motivation

Background: Block Copolymers Basics

- *Block copolymers* (BCPs): two or more chemically distinct polymers bonded together (e.g., *AB*, *ABC*, *ABA*, etc.).

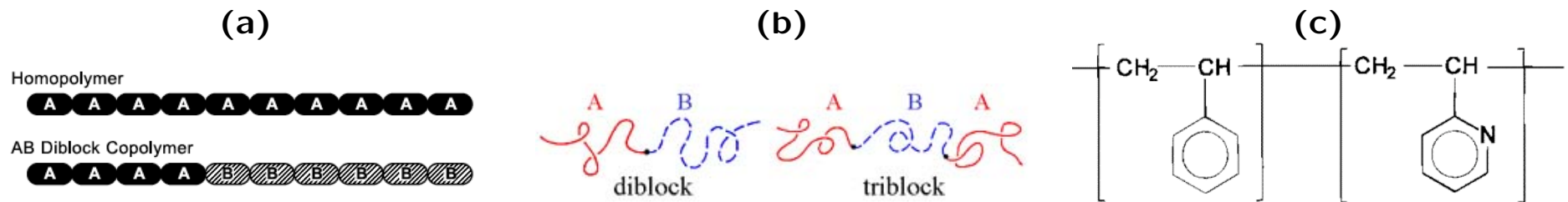


FIG 1: (a) Schematic of a homopolymer and a BCP*, (b) example BCPs†, and (c) schematic of poly(styrene-*b*-2-vinylpyridine) (PS-PVP).

*Fredrickson, *The Equilibrium Theory of Inhomogeneous Polymers* (Clarendon Press, Oxford, 2006).

†<http://www.princeton.edu/~polymer/block.html>.

- The distinct segments are often chemically immiscible: free-energy cost per segment of contacts between I and J segments $\chi_{IJ} > 0$.
- Competition between Hookian, entropic restoring force and energetic tendency to separate segments induces *microscopic phase separation*.
- *Microphase separation* or *mesophase separation*: like oil and water on $\mathcal{O}(10 \text{ nm})$ scale!

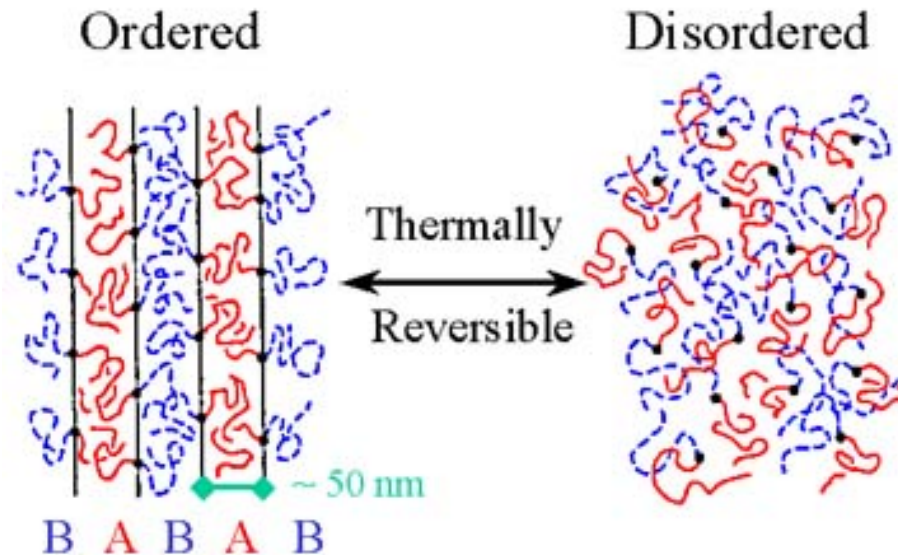


FIG 2: Schematic of mesophase separation*.

*<http://www.princeton.edu/~polymer/block.html>.

- For AB diblocks, where $f_A = f$ is the fraction of A segments, the specific mesophase is determined by f and $\chi_{AB}N = \chi N$, where N is the copolymer index of polymerization (i.e., the total number of segments along the copolymer backbone):

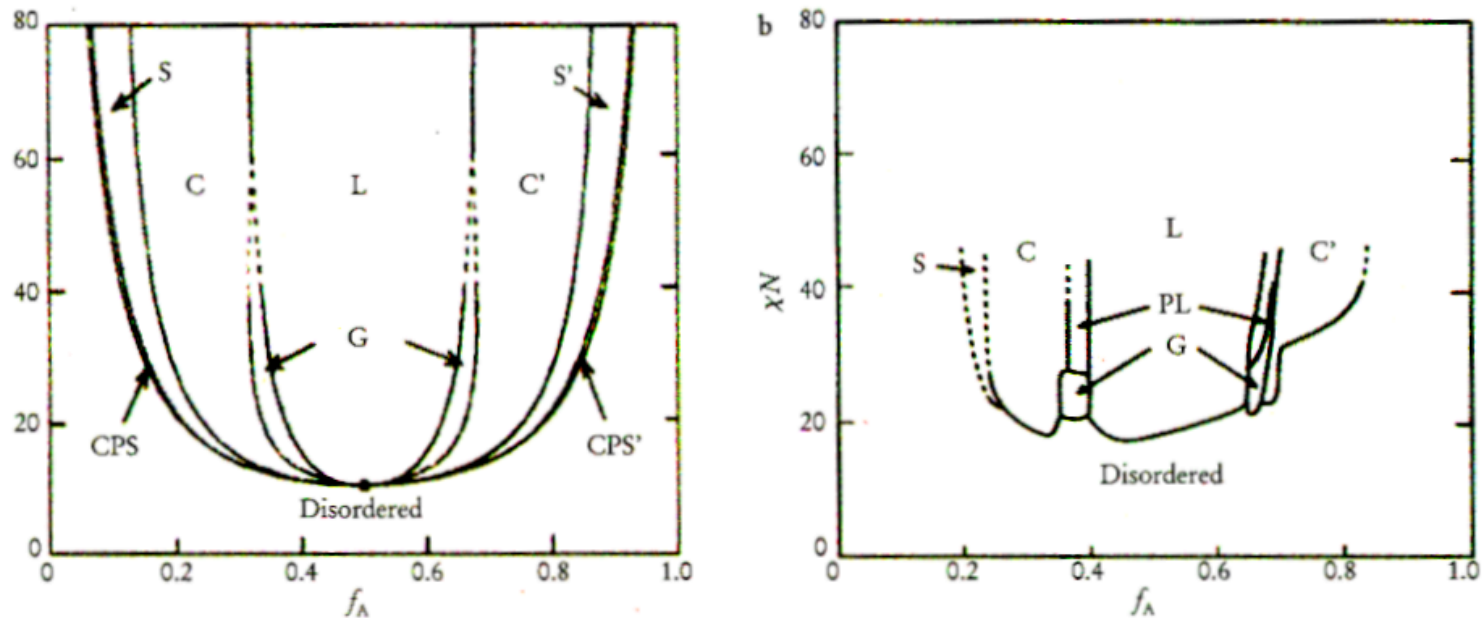


FIG 3: (LEFT) Theoretical (mean-field) mesophase diagram for a 3D AB diblock copolymer system, and **(RIGHT)** experimental mesophase diagram for a 3D AB diblock system*.

*Bates & Fredrickson, *Physics Today*, February 1999.

Motivation: BCP Resists*

- BCP thin films are being considered for resist applications in next-generation electronics and bit-patterned media nanofabrication.

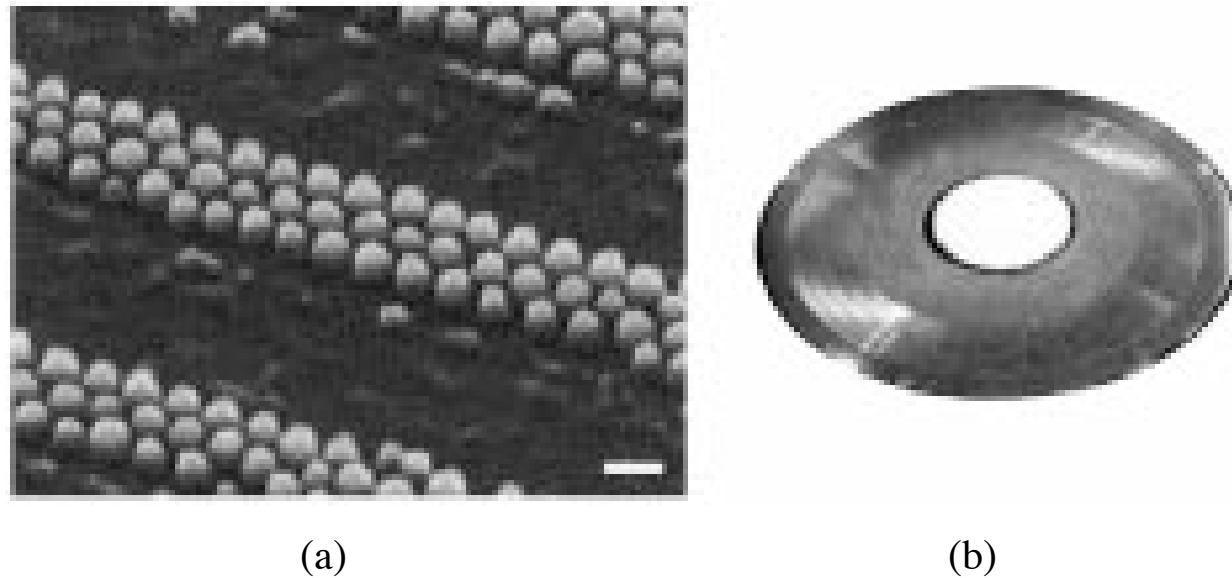


FIG 4: (a) SEM image of the patterned magnetic medium ($\text{Co}_{74}\text{Cr}_6\text{Pt}_{20}$) with a 40-nm diameter. The scale bar indicates 100 nm. (b) Whole image of the patterned media disk prepared on a 2.5-inch HDD glass plate. (Figure and caption from Naito et al., 2002.[†])

*Reviews: Park, Yoon, & Thomas, *Polymer* **44**, 6725 (2003); Segalman, *Mater. Sci. Eng. R* **48**, 191 (2005); Darling, *Progress in Polymer Science* **32**, 1152 (2007).

[†]Naito et al., *IEEE Transactions on Magnetics* **38**, 1949 (2002).

- How BCP lithography works:

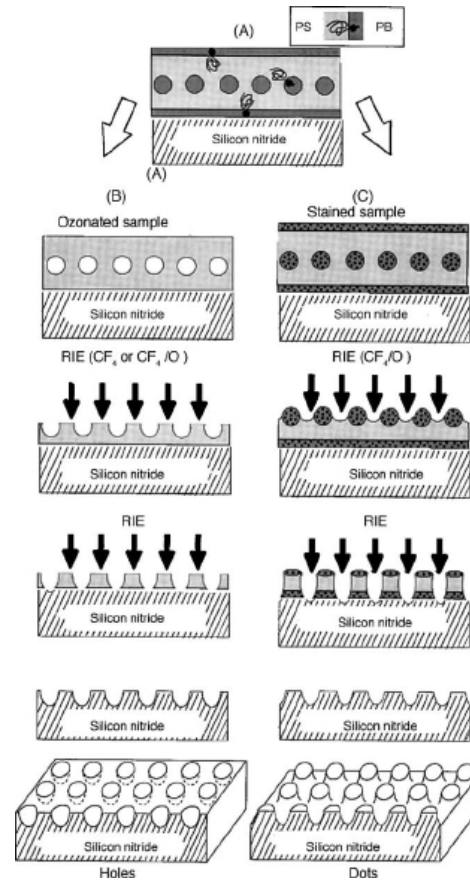


FIG 5: Schematic of the BCP lithography process.*

*Figure from Segalman, *Mater. Sci. Eng. R* **48**, 191 (2005)

- Resist applications demand *significant* control over microdomain ordering:

*“Further study is necessary to obtain a uniform dot diameter and regular dot position. ... Fluctuations in the size and position of the patterned cell, observed for the present media, should be reduced for the realization of patterned media.”**

- Template-directed self assembly (TDSA) shows considerable promise for controlling microdomain order in BCP systems.

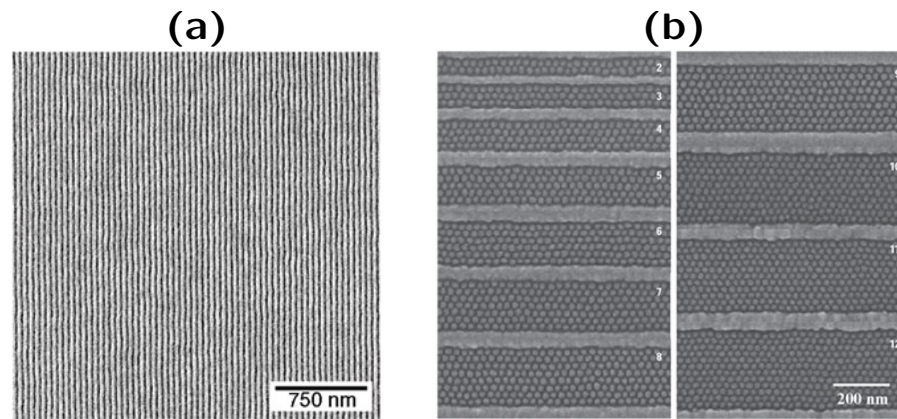


FIG 6: (a) Chemically templated diblock copolymer thin film.[†] (b) Topographically templated diblock copolymer thin films.[‡]

- International Technology Roadmap for Semiconductors (ITRS) includes TDSA of BCPs, and it sets limits on placement errors, interfacial fluctuations (line edge roughness [LER]), and width fluctuations (line width roughness [LWR]).

*Naito et al., *IEEE Transactions on Magnetics* **38**, 1949 (2002).

[†]Kim et al., *Nature* **424**, 411 (2003)

[‡]Cheng, Mayes, & Ross, *Nature Materials* **3**, 823 (2004)

- However, LER/LWR is obvious even in well-ordered BCPs:

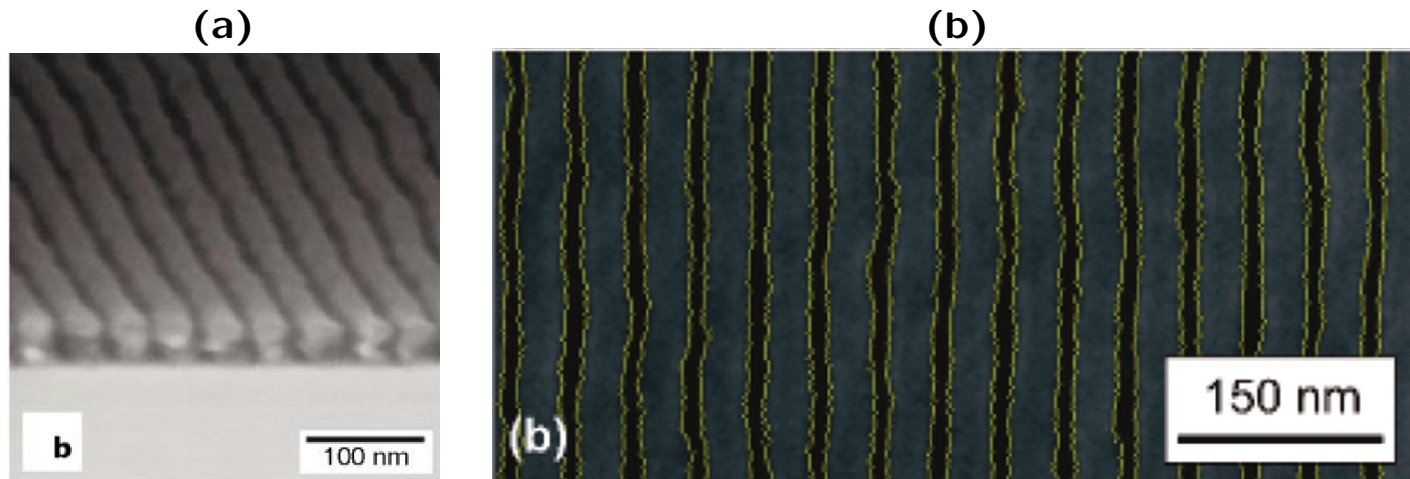


FIG 7: Chemically templated PS-*b*-PMMA diblock copolymer thin films from (a) P. Nealey* and (b) G. Stein.†

- It is not yet clear if BCP systems will satisfy the necessary LER/LWR requirements! A better fundamental understanding of BCP LER/LWR is necessary, and high-quality measurements of real systems are needed.

Here we discuss phase-field simulation of LER and LWR in block copolymer melts.

*Kim et al., *Nature* **424**, 411 (2003).

†Stein et al., *Macromolecules* **43**, 433 (2010).

Measuring and Modeling Interfacial Fluctuations in BCP Resists

- The *Dimensional Metrology for Nanofabrication* project in the NIST Polymers Division has an established and growing effort on the dimensional metrology of nanofabrication-relevant polymer systems, including nanoimprint systems, traditional photoresist systems, *and* BCP systems.
- Our effort is largely focused on developing scattering techniques (e.g., SAXS, SANS, GISAXS, etc.).
- Analysis of scattering data requires an understanding of the underlying physics and often requires detailed models.
- Our modeling and simulation efforts are geared towards advancing fundamental understanding of BCP resist materials *and* developing/improving scattering models for BCP resists.

- LER models can be separated into three classes:
 1. **Capillary wave models.**
 - Convolve capillary interface with mean-field interfacial profile.*
 - Implicitly assume that the capillary wavelength is much larger than interfacial width (i.e., SSL).
 2. **Weak segregation limit (WSL) models**
 - Ordered-phase random phase approximation.†
 - Analytically intractable, but “correct” treatment of fluctuations in WSL.
 3. **Simulations** (can be thought of as model independent, in some sense)
 - Particle-based, field-theoretic, etc.‡
 - Fluctuations are “intrinsic,” no assumptions beyond the basic polymer models.
 - Can often examine a range of segregation strengths.
 - Results still need to be interpreted ... (other models are often used in this context)
- We have elected to initially focus on simulations with the goal of refining and/or developing scattering models based on the simulation findings.

*Semenov, *Macromolecules* **26**, 6617 (1993).

†Yeung et al., *Macromol. Theory Simul.* **5**, 291 (1996).

‡Grisinger, Muller, & Binder, *J. Chem. Phys.* **111**, 5251 (1999); Srinivas, Swope, & Pitera, *J. Phys. Chem. B* **111**, 13734 (2007); Bosse et al., *Soft Matter* **5**, 4266 (2009).

- In this context, simulation frameworks can be separated into three classes:
 1. **Particle-based**
 - E.g., Molecular Dynamics, Monte Carlo, etc.
 - Optimized for short-wavelength physics.
 - Can be applied to large-scale systems, but very computationally demanding.
 2. **Field-theoretic**
 - E.g., SCFT-based approaches.
 - Particle-based, but optimized for mesoscale.
 - Computationally demanding for high-resolution or large-scale simulations.
 3. **Phase-field**
 - E.g., Leibler-Ohta-Kawasaki (LOK), Brozovskii-Fredrickson-Helfand, etc.
 - Optimized for long-wavelength physics (i.e., $>$ interface width).
 - LOK framework can cover all segregation strengths.
 - Amenable to analytic evaluation and large-scale numerical simulation.
- The ITRS has singled out long-wavelength LER/LWR (i.e., wavelengths longer than the critical dimension) as especially troublesome for TDSA resists. This is precisely the “sweet spot” for phase-field simulations.

Phase Field Simulations

- Following Ohta and Kawasaki,^{*} we express the AB diblock copolymer free energy in a Landau form:

$$H[\phi] = \int d\mathbf{x} \left[\frac{\delta^2}{2} (\nabla\phi)^2 - \frac{1}{2}\phi^2 + \frac{1}{4}\phi^4 \right] + \frac{\sigma}{2} \int d\mathbf{x} \int d\mathbf{x}' \frac{[\phi(\mathbf{x}) - \bar{\phi}][\phi(\mathbf{x}') - \bar{\phi}]}{4\pi|\mathbf{x} - \mathbf{x}'|}, \quad (1)$$

where $\bar{\phi} = 1 - 2f$; f is the fraction of A segments along the diblock; δ and σ are phenomenological *coupling constants*; and $\phi = \phi_B - \phi_A$, where ϕ_A and ϕ_B are the local fractions of A and B segments, respectively.

- The parameter δ is proportional to the interfacial width, and thus $\delta \sim \chi^{-1/2}$.
- The parameter σ scales like $\sigma \sim N^{-2}$.
- In order to examine fluctuations in this model, we perform a stochastic field update:

$$\frac{\partial\phi}{\partial t} = \nabla^2 \frac{\delta H}{\delta\phi} + \zeta, \quad (2)$$

where ζ is a random noise term that obeys the fluctuation dissipation theorem.

- Following a rescaling of variables, the two parameters of interest are:
 1. Quench depth: $\tilde{\delta} \equiv \sqrt{\sigma}\delta \sim 1/(\chi N)$.[†]
 2. Noise strength: $\epsilon \equiv (2\sigma^{d/2})^{1/2}$, where d is the spatial dimension.

^{*}Ohta and Kawasaki, *Macromolecules* **19**, 2621 (1986)

[†]Liu and Goldenfeld, *Physical Review A* **39**, 4805 (1989); Choksi, Peletier, and Williams, *SIAM J. Appl. Math.* **69**, 1712 (2009).

Results

Proof of Concept

- First, a few simulations to test that things are working like we'd expect.
- We used an external “pinning field” at $y = 0$ and $y = L_y$ to help orient the microdomains.

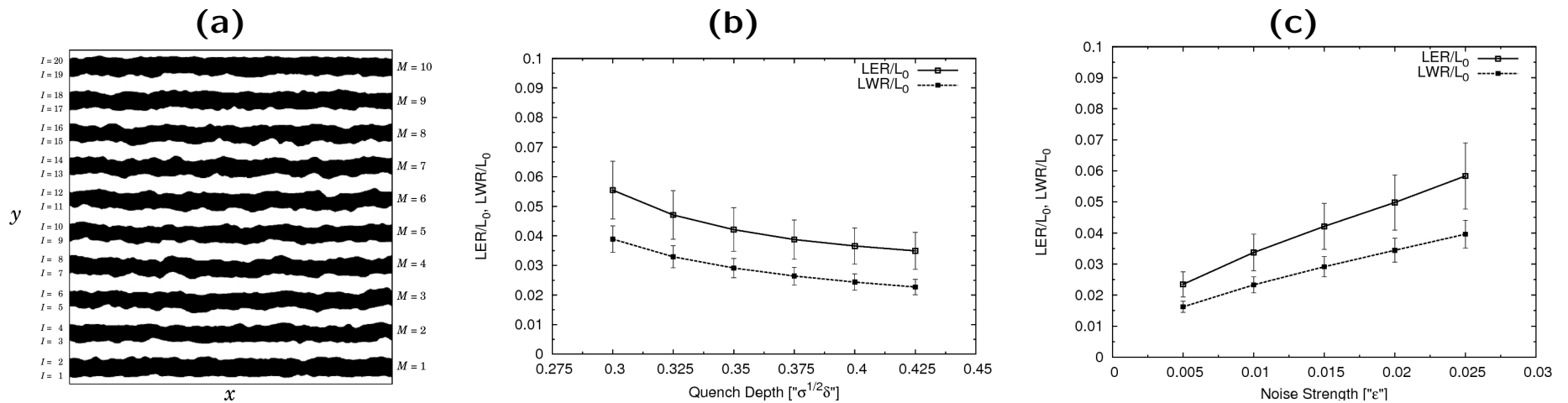


FIG 8: $f = 0.5$ and other coupling constants set for WSL. Plots of (a) ϕ_A ; (b) LER/L_0 , LWR/L_0 vs. Quench Depth for the center microdomain in (a); and (c) LER/L_0 , LWR/L_0 vs. Noise Strength for the center microdomain in (a). Here LER and LWR are the “one sigma” definitions, and L_0 is the interdomain spacing.

- Results are consistent with our intuition. Deeper quenches and less noise (i.e., larger N) yield less LER/LWR.

Some Interesting Results

- The LER and LWR spectra are non-trivial:

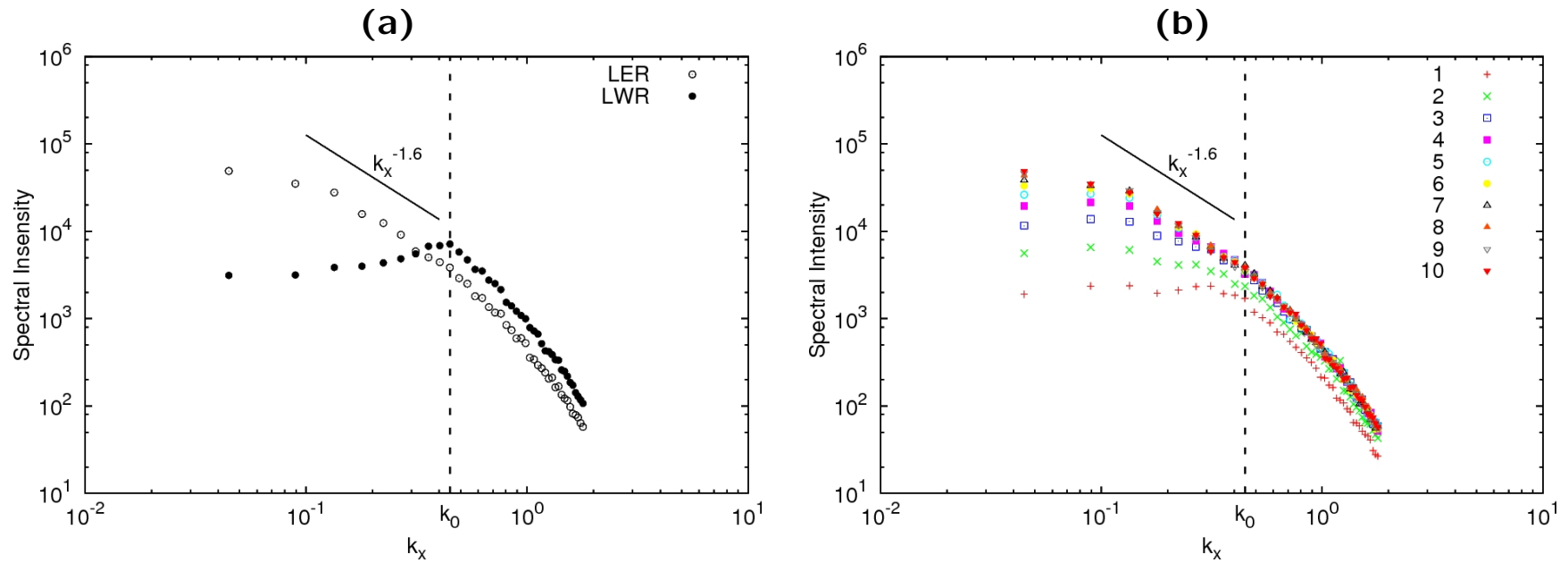


FIG 9: $f = 0.5$ and other coupling constants set for WSL. Plots of **(a)** LER and LWR spectra; and **(b)** LER spectra for interfaces $I = 1$ through $I = 10$, where the $I = 1$ interface is nearest the pinning field at $y = 0$.

- Note the shoulder/peak in the LER/LWR spectra at $k_0 = 2\pi/L_0$ and the non-capillary-like $k^{-1.6}$ scaling in the long-wavelength ($< k_0$) LER spectra. This suggests that long-wavelength LER/LWR has a characteristic wavelength *and* is generally non-capillary-like. $k^{-1.6}$ scaling is consistent with recent SEM measurements*
- In Fig. 9b we see that the pinning field at $y = 0$ can significantly suppress long-wavelength LER—this is technologically important. While “intrinsic” LER could present a problem, external fields can be used to suppress long-wavelength LER.

*Stein et al., *Macromolecules* **43**, 433 (2010).

Some Preliminary Results

- LER and LWR spectra for weakly segregated and strongly segregated melts:

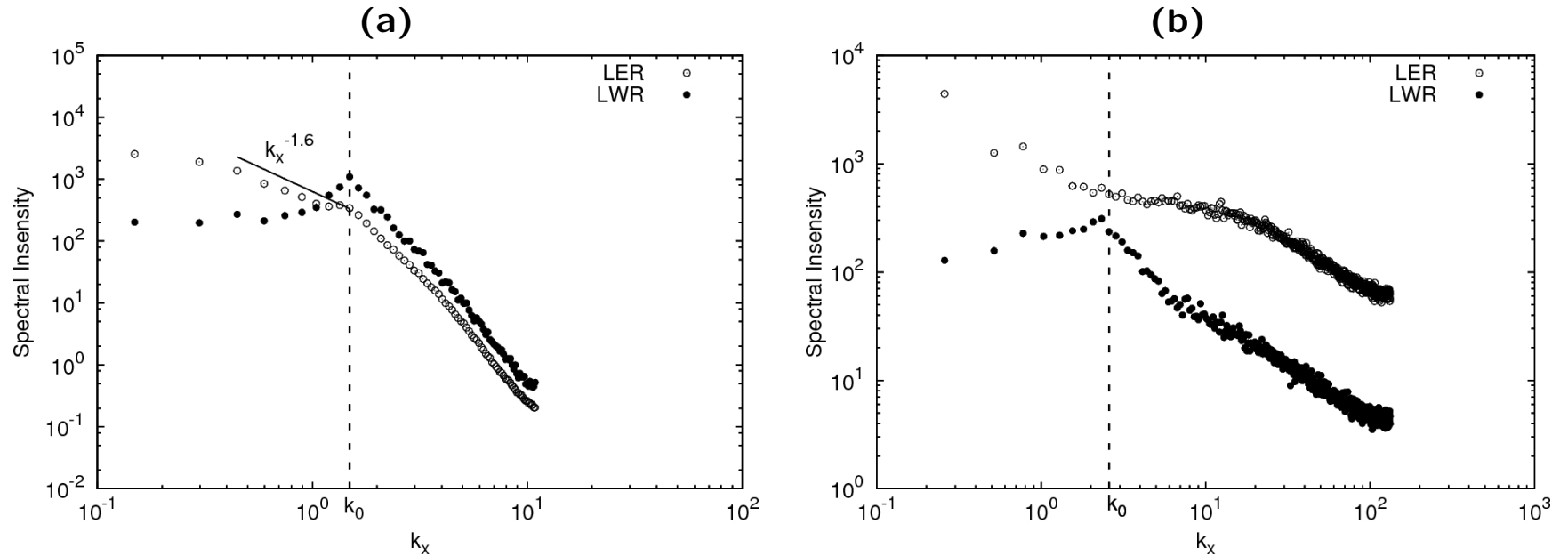


FIG 10: $f = 0.5$. Plots of **(a)** LER and LWR spectra for weakly segregated system (i.e., sine wave composition profile); **(b)** LER and LWR spectra for intermediate to strongly segregated system (i.e., square wave composition profile).

- Fig. 10a is similar to the previous slide (both systems were weakly segregated); however, the SSL spectra presented in Fig. 10b is both qualitatively and quantitatively different from Figs. 9 and 10a. Further modeling and simulation work is necessary.

Remarks

- Phase-Field framework is a powerful tool for simulating long-wavelength LER/LWR in BCP resists.
- LER/LWR has a characteristic wavelength L_0 .
- Long-wavelength LER does *not* appear to scale like capillary waves.
- Pinning field locally suppresses long-wavelength LER—technologically important.
- Large-scale simulation can be used to interpret scattering measurements, evaluate existing scattering models, and draft new scattering models.
- Here $\text{LER} > \text{LWR}$ —suggests interfaces are correlated.
- LER in SSL does not appear to be capillary-like.
- LWR in SSL retains peak at L_0 —important for modeling.

Acknowledgments

- Eric Lin (NIST), Wen-li Wu (NIST), Ron Jones (NIST), Chris Soles (NIST), Gila Stein (NIST and University of Houston) and Kevin Yager (NIST and Brookhaven) for helpful discussions.

